First demonstration of the use of crab cavities on hadron beams

R. Calaga[1,*] A. Alekou,[2] F. Antoniou,[1] R. B. Appleby,[2] L. Arnaudon,[1] K. Artoos,[1] G. Arduini,[1]
V. Baglin,[1] S. Barriere,[1] H. Bartosik,[1] P. Baudrenghien,[1] I. Ben-Zvi,[3] T. Bohl,[1] A. Boucherie,[1]
O. S. Brüning,[1] K. Brodzinski,[1] A. Butterworth,[1] G. Burt,[4] O. Capatina,[1] S. Calvo,[1] T. Capelli,[1]
M. Carlà,[1] F. Carra,[1] L. R. Carver,[5] A. Castilla-Loeza,[4] E. Daly,[6] L. Dassa,[1] J. Delayen,[7]
S. U. De Silva,[7] A. Dexter,[4] M. Garlasche,[1] F. Gerigk,[1] L. Giordanino,[1,8] D. Glenat,[1]
M. Guinchard,[1] A. Harrison,[1] E. Jensen,[1] C. Julie,[1] T. Jones,[9,4] F. Killing,[1] A. Krawczyk,[10]
T. Levens,[1] R. Leuxe,[1] B. Lindstrom,[1] Z. Li,[11] A. MacEwen,[6] A. Macpherson,[1] P. Menendez,[1]
T. Mikkola,[1] P. Minginette,[1] J. Mitchell,[1,4] E. Montesinos,[1] G. Papotti,[1] H. Park,[6] C. Pasquino,[1]
S. Pattalwar,[9] E. C. Pleite,[1] T. Powers,[6] B. Prochal,[10] A. Ratti,[11] L. Rossi,[1] V. Rude,[1]
M. Therasse,[1] R. Tomás,[1] N. Stapley,[1] I. Santillana,[1] N. Shipman,[1,4] J. Simonin,[1] M. Sosin,[1]
J. Swieszek,[1] N. Templeton,[9] G. Vandoni,[1] S. Verdú-Andrés,[3] M. Wartak,[10]
C. Welsch,[5] D. Wollman,[1] Q. Wu,[3] B. Xiao,[3] E. Yamakawa,[4] C. Zanoni,[1]
F. Zimmermann,[1] and A. Zwozniak[10]

[1]*CERN, CH-1211 Geneva 23, Switzerland*
[2]*The University of Manchester and the Cockcroft Institute, Manchester, M13 9PL, United Kingdom*
[3]*Brookhaven National Lab, Upton, New York, USA*
[4]*Lancaster University, Cockcroft Institute, LA1 4YR Lancaster, United Kingdom*
[5]*The University of Liverpool, Cockcroft Institute, L69 7ZE Liverpool, United Kingdom*
[6]*Jefferson Lab, Newport News, Virginia 23606, USA*
[7]*Old Dominion University, Norfolk, Virginia, USA*
[8]*Kraftenlagen Assystem Consortium, CH-1211 Geneva 23, Switzerland*
[9]*STFC, Daresbury Laboratory, Warrington, WA4 4AD, United Kingdom*
[10]*Institute of Nuclear Physics PAN, 31-342 Kraków, Poland*
[11]*SLAC, National Accelerator Laboratory, Menlo Park, California 94025, USA*

Many future particle colliders require beam crabbing to recover geometric luminosity loss from the nonzero crossing angle at the interaction point (IP). A first demonstration experiment of crabbing with hadron beams was successfully carried out with high energy protons. This breakthrough result is fundamental to achieve the physics goals of the high luminosity LHC (HL-LHC) and the future circular collider (FCC). The expected peak luminosity gain (related to collision rate) is 65% for HL-LHC and even greater for the FCC. Novel beam physics experiments with proton beams in CERN's Super Proton Synchrotron (SPS) were performed to demonstrate several critical aspects for the operation of crab cavities in the future HL-LHC including transparency with a pair of cavities, a full characterization of the cavity impedance with high beam currents, controlled emittance growth from crab cavity induced rf noise.

Particle colliders are important engines of discovery, and collisions between both protons and leptons have shone a light on the fundamental structure of our universe for decades. These colliders operate by the acceleration, subsequent manipulation and finally collision of charged particle beams. The beam manipulation at the IP of the

beams is crucial to create optimal collision conditions and maximise the rate of collisions over several hours and in multiple IPs around the ring.

In the Large Hadron Collider (LHC) [1] and most future colliders such as FCC [2] and EIC [3], the bunch spacing, magnetic optics and physical constraints to confine the collisions only at the IP require a configuration with beam crossing (or crossing angle) to physically separate the beams immediately before and after the collision. Particle bunches in colliders are generally significantly longer than their transverse width at the IP. In the LHC luminosity upgrade (HL-LHC) [4], the bunches are 4 orders of magnitude longer than the transverse size. This large

*[*]rama.calaga@cern.ch

aspect ratio combined with the finite crossing angle reduces the overlap between the colliding bunches, and hence reduces the number of collisions or, equivalently, the luminosity [5]. The luminosity reduction factor for Gaussian bunches is given by,

$$R_\phi = (1 + \phi^2)^{-1/2}, \qquad (1)$$

where $\phi = \theta\sigma_z/2\sigma_x$ is the Piwinski angle, θ is the crossing angle and σ_z/σ_x is the ratio of the longitudinal and transverse size of the bunch [6]. For the present LHC, the Piwinski angle is $\phi = 0.65$ while for HL-LHC it is $\phi = 2.66$ showing the steep reduction in the peak luminosity of 65% or higher of the total available luminosity.

An elegant scheme to transversely the bunches before and after the collision point to recover the optimum overlap between the colliding bunches is achieved using rf crab cavities. Originally proposed for linear colliders, these rf cavities impart a time-dependent electromagnetic transverse kick to the particle bunches which is referred to as a geometric compensation of luminosity loss for colliders [7]. The kick is transformed to a relative displacement of the head and the tail of the bunch at the IP to impose a head-on collision which is schematically illustrated in Fig. 1. This concept was later extended to circular colliders [8].

In circular colliders, a local crab compensation scheme introduces a localized perturbation upstream of the concerned IP and compensates for it downstream, such that through the rest of the ring the bunches remain unperturbed. A full crab compensation in HL-LHC requires a kick voltage of up to 9 MV per beam per side of each collision point [3,9]. In order to sustain such high surface electromagnetic fields in continuous wave (CW), superconducting rf cavities are essential. The first operational crab cavities used superconducting technology at a 508.9 MHz in the KEKB $e^+ - e^-$ collider at KEK in Japan [10]. The frequency choice is primarily driven by the length of the proton bunches. The finite rf curvature represents an additional reduction factor in the luminosity. For the specific case of HL-LHC, it was shown that a frequency of 400 MHz and for a wide range of transverse beam sizes at the IP, this reduction factor is close to unity [11]. Very tight transverse space constraints in the HL-LHC triggered the development of novel and compact rf deflecting structures.

Crab cavities are in the baseline of future collider projects. However, crab cavities were never operated with hadron beams and the crab manipulation has never been demonstrated on hadron bunches and there are key beam

physics questions that must be investigated. Proton bunches are typically much longer than electron bunches leading to lower frequencies and complex bunch shapes. Synchrotron radiation damping is significantly weaker for hadrons and emittance [12] growth due to rf noise and wakefields may limit luminosity gain. In this paper we present the first experimental demonstration of a crab cavity with a hadron beam, performed in the SPS at CERN to analyze these effects. Several key beam dynamics aspects of proton beams in the presence of crab cavities are addressed opening the door to transverse crabbing of proton beams in most future accelerators. A compact crab cavity geometry, which is four times smaller than the KEK-B cavity scaled to the same frequency, "double quarter wave" (DQW), was also demonstrated [13–15]. The cavity and its electromagnetic fields is shown in Fig. 2. Such transversely compact cavities reaching very high voltages are the enabling technology to implement crab crossing in the HL-LHC and future colliders.

Two superconducting prototype DQW-type crab cavities manufactured at CERN underwent rf tests in a super-fluid helium bath at a temperature of 2 K. These first cavity tests demonstrated a maximum transverse-kick voltage exceeding 5 MV, surpassing the nominal operational voltage of 3.4 MV [16].

These two identical DQW cavities were inserted into a specially designed cryostat under ultra high vacuum to reduce the cryogenic heat load and also to shield from stray magnetic fields [17,18]. The position of each cavity inside the cryomodule is measured by an optical system based on frequency scanning interferometry (FSI) system [19]. From FSI measurements, the mechanical centers of the two cavities were found to be displaced with respect to each other by less than 200 μm compared to the specification of 500 μm. A "slow" mechanical tuning system is used to control the cavity frequency to be synchronous to a harmonic of the beam revolution frequency [20,21].

During 2018, a total of 7 sessions of the SPS accelerator time, known as machine developments (MDs), each 10 hours long were dedicated to measurements with the crab cavities. The SPS operates with a repeating master

FIG. 1.   Bunches colliding with a crossing angle without crab crossing (left); with the crab crossing (right).
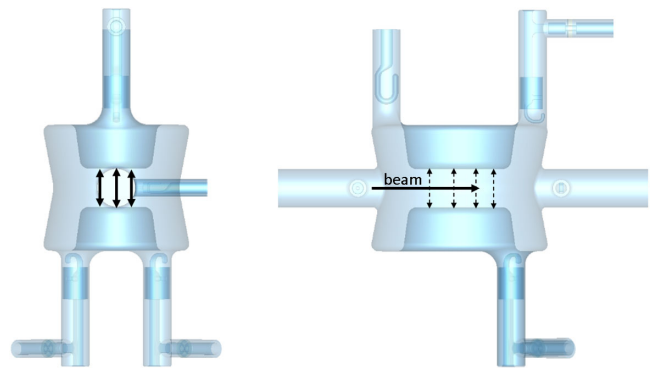

FIG. 2.   Cross section views of the vertical DQW cavity and coupler design used for the beam tests in the SPS.

cycle with embedded subcycles to provide beams to different users including crab cavity MDs. At the beginning of each cycle, the rf frequency of the accelerating cavities in the SPS operating at 200 MHz must become synchronized with the crab cavity frequency operating at 400 MHz. The two rf systems are physically separated in the SPS ring by approximately 3 km. Due to the large bandwidth of the accelerating rf system of the SPS, a fixed crab cavity frequency is used as a master and sent to the accelerating cavities' control system via a phase compensated fiber optical link to re-synchronize the beam. The crab cavities' voltage was then ramped up to the operating level once this synchronization is completed.

Shortly after the first injection of protons, the crab cavity—SPS frequency synchronization was operational and the first static crabbing of a proton beam could be measured at a transverse voltage of 1 MV. To precisely measure the crabbing signal, a static orbit offset is removed from a reference signal acquired before the rf synchronization becomes active [22]. The equivalent crab cavity voltage measured by the head-tail (HT) monitor [23] was calculated from the focusing configuration of the SPS magnetic elements (also known as magnetic optics) and the measured intra-bunch offsets. A comparison of the intrabunch transverse displacement of a single bunch is seen in Fig. 3, which shows the particle density for several cases; crab cavities switched off (left) and synchronous crabbing coming from two crab cavities in phase (center), demonstrating clearly the transverse (y)—longitudinal(t) correlation.

The use of the crab cavities for HL-LHC also requires that during the injection, energy ramp or operation without crab cavities, the cavities remain transparent to the beam, known as "crabbing off." Since more than one cavity is used, counterphasing (such that the relative cavity rf phase $= \phi_1 - \phi_2 = \pi$) reduces the effective kick voltage to zero while always keeping accurate control of the cavity field. This scheme is also most effective for beam stability and was successfully demonstrated as shown in Fig. 3 (right). The counterphasing of two crab cavities 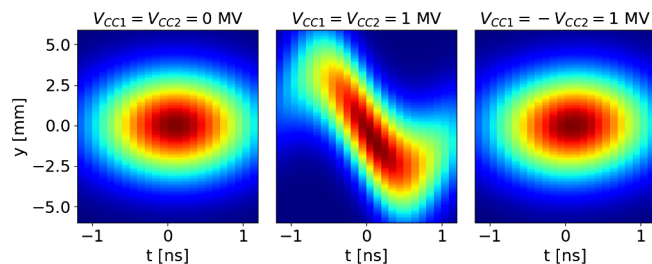was successfully demonstrated in the SPS beam tests. Each cavity was individually powered to $V_1 = V_2 = 1$ MV and set as close to the crabbing phase as possible ($\phi_1 = \phi_2 = 0$). The measured bunch tilt for three different cases is seen in Fig. 3, the left plot shows the beam with both the crab cavities held at zero voltage, cavities in-phase and at $V = 1$ MV in the middle plot, and the right plot showing the cancellation effect between the two cavities when the cavities are counterphased. This is the first demonstration to make crab cavities invisible to a hadron beam when not in use and an essential step for the operation of crab cavities in colliders such as the HL-LHC. The strong rf curvature in the longitudinal plane where both cavities are in-phase matches exactly to the 400 MHz rf wave with no measurable negative effects on beam quality and lifetime compared to that of the case with the cavities off. The bunch tilt was measured to be 17 mrad, which is a good match to the expected 400 MHz sinusoidal shape at $V = 1$ MV. The crabbing was cancelled between two cavities to the level of approximately 60 kV, which is the limit of the tilt measurement in the HT monitor.

The longitudinal impedance of the operating mode of these cavities vanishes on axis, i.e., there is no beam loading for a centered beam; the rf generator does not exchange energy with the beam [24]. For a beam circulating at an offset Δx, the beam-induced voltage is proportional to the offset and average beam current. Therefore, the electrical center was inferred by scanning the beam in the transverse plane and measuring the zero-crossing of the induced voltage. First measurements were carried out in the vertical plane for the DQW cavities with 2 batches of 24 bunches spaced by 25 ns and a gap space of 225 ns, like in the LHC, with a bunch intensity of 1×10^{11} p/b. Figure 4 shows that the electrical centers are well within the specified tolerance and close to the theoretical

FIG. 3. Intra-bunch motion from three different cases measured with the HT monitor. Left: crab cavities switched off (voltage $= 0$). Center: synchronous crabbing with both cavities in phase corresponding to $V_{CC} \approx 2$ MV total voltage ($V_{CC1} = V_{CC2} = 1$ MV). Right: cavities in counterphase, corresponding to residual $V_{CC} \approx 60$ kV total voltage.
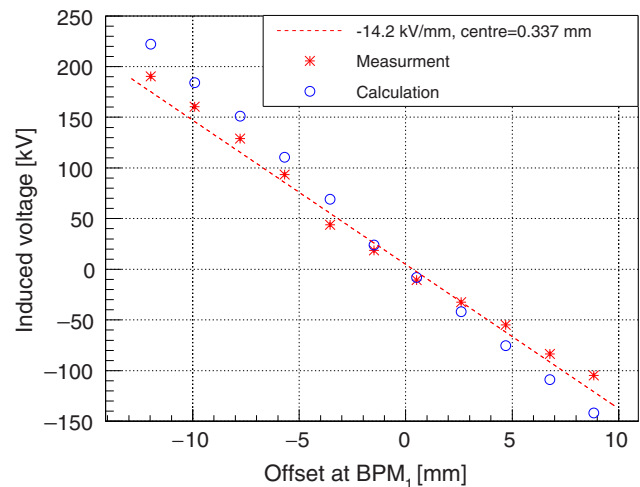

FIG. 4. Beam loading measurements as a function of beam offset for cavity 1 compared to expected values. The electrical center is similar for cavity 2 and within the specified tolerance of $\leq 500~\mu$m [3].

values [25]. This was independently confirmed by the FSI survey measurements.

In the HL-LHC, a single frequency reference generated at the rf controls of the accelerating cavities will be sent over phase-compensated links to respective crab cavities at IP_1 and IP_5 to synchronize the crab cavities with the beam. An amplitude jitter in the crab cavity voltage introduces a residual crossing angle at the IP and a phase jitter in the cavity voltage results in a transverse offset at the IP. The impact of rf noise on emittance and luminosity was experimentally studied with e^+e^- beams in SKEKB [26].

The emittance growth induced by rf noise is of particular concern with proton beams, which have very low synchrotron radiation damping and long physics fills. For example, first performance estimates in HL-LHC with realistic crab cavity amplitude and phase noise yield about a 2% luminosity loss [27]. The amplitude and phase control must be achieved also during filling and energy ramping with small (or zero) field in the cavities in the presence of beam loading. Smooth transition between no-crabbing and crabbing must be realized prior to collisions, as demonstrated during the transparency test.

The 270 GeV cycle in the SPS was used to study the effect on the emittance growth and predict the requirements on the rf feedback for amplitude and phase noise. At 270 GeV, the beam in the SPS can be maintained for extended periods (several hours) with proton bunches very close to properties of the bunches injected into the HL-LHC. A single low intensity proton bunch is used to minimize all other mechanisms of emittance growth in the SPS with a residual growth of approximately 5 μm h^{-1} [28]. Controlled amplitude and phase noise up to 10 kHz was injected into the rf feedback to overlap with the betatron sideband at 7.74 kHz. Emittance measurements using the SPS wire scanners [29] were made with varying noise levels and compared to predictions [30] as shown in Fig. 5. The relative emittance growth with an injected phase noise of −110 dBc/Hz was measured to be 1.75 μm per hour. The measured amplitude noise is approximately 10 dB below the phase noise at the betatron sideband.

The emittance growth scaling with noise level increases similar to the theoretical estimates while the measured growth rate is consistently a factor of 2-3 lower than the predicted values. The agreement of the scaling with theoretical estimates allows to put an upper bound of approximately −143 dBc/Hz on the required rf phase noise specification for HL-LHC. Further experiments will be conducted to investigate the sensitivity of the emittance growth to the bunch length, bunch longitudinal distribution, crab cavity voltage, impedances and the impact of the phase offset between the crab cavities and the accelerating system to understand the discrepancy. These measurements allows us to put an upper bound on the required rf phase noise specification for
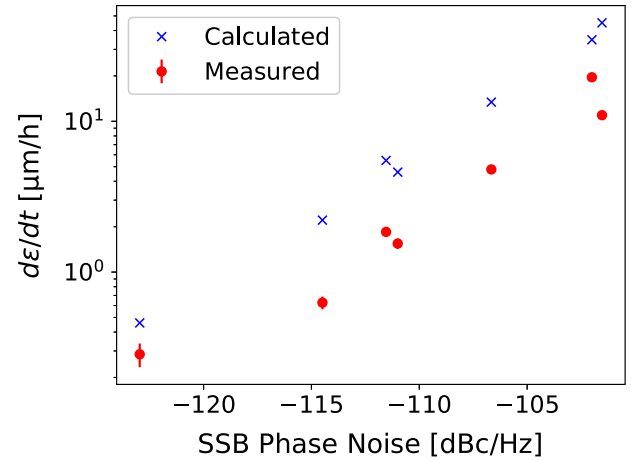

FIG. 5. Emittance growth measurements as a function of single sideband (SSB) phase noise injected into the cavity feedback on a logarithm scale.

HL-LHC which could be relaxed by approximately 10 db with respect to the initial estimates.

On resonance, the large impedance of the fundamental deflecting (dipole) mode is canceled between the positive and negative sideband frequencies, which are symmetric around main rf frequency, ω_{rf}. The active feedback will reduce the impedance and hence the growth rates by a large factor.

For higher order modes (HOMs) in HL-LHC, the cavities equipped with HOM couplers were carefully designed to keep the impedance within tight tolerances, and the system remains close to the limits [3,31,32]. As such the SPS test aimed to verify that the impedance was in good agreement with the simulated values. The DQW cavity uses three on-cell HOM couplers mounted in the vertical plane and a mushroom-shaped antenna on the cavity beam pipe to meet the impedance specifications [14,15].

Dedicated measurements of the HOMs were carried out in the SPS for different beam parameters and bunch filling schemes. Figure 6 shows the measured power as a function of frequency over the broad range of 0.5–2.0 GHz where the upper limit is chosen at the beam pipe cut-off frequency. In the SPS, the longitudinal line density of the bunch is best represented by a binomial distribution. The fitted distribution of the longitudinal bunch profile measurements yield the exponent term $\mu = 1.5$ and a full width half maximum bunch length of 1.06 ns. Using these parameters, a good overall agreement between the measured HOM spectrum and simulation was observed over this large frequency range.

Some discrepancies in the measured amplitude peaks could arise due to the lack of the exact distribution of the power at each discrete frequency through the three HOM couplers on the DQW cavity. In simulations the power is assumed to be equally distributed. The large discrepancy at 1800 MHz is caused due to a mismatched termination on
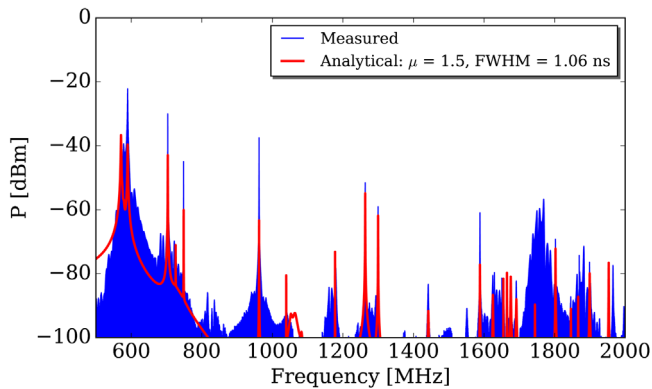
FIG. 6. Measured HOM power vs frequency, comparing measured data (blue) and simulated values (red).

the field antenna in presence of a rf filter needed for the fundamental mode signal. The highest contributor to the HOM power is the longitudinal mode at 960 MHz. The majority of this power ($>98\%$) couples to the top HOM coupler and remains below the 1 kW threshold for the HL-LHC parameters (see Table I). This mode is close to a node of the binomial distribution in the frequency domain. Therefore, the calculated spectral power is sensitive to the exact frequency value and the longitudinal bunch profile. A stochastic study of the calculated HOM power for both binomial and Gaussian distributions using measured cavity impedance are in all cases within the threshold of 1 kW except for a worst case scenario being 8% over the threshold which is acceptable. For the transverse plane, the power induced in the lowest frequency mode at 748 MHz was measured as a function of the beam offset. The measured power with beam offset was identical to the simulated results. These detailed impedance measurements are analyzed with proposals for improvements in HOM damping for HL-LHC in Ref. [33]. Due to the compact nature of the crab cavity design, a strong nonlinear component of deflecting field (skew sextupole) is expected which could have a

negative impact on the beam dynamics of the HL-LHC. During the beam-based experimental measurements, the skew sextupolar component was measured to be within an acceptable range for the HL-LHC [34,35].

Many future particle colliders require crab cavities to align bunches for collision at the IP. These cavities have previously been demonstrated on electron beams and in this paper we have shown, for the first time, the crabbing action of crab cavities on hadron beams. We have demonstrated this first crabbing of a proton beam in the SPS superconducting rf test stand at CERN with a transverse voltage of 1 MV per cavity. The transverse beam manipulation was measured with a HT monitor. It was possible to drive both cavities in counterphase to demonstrate that the cavities can be made transparent to the beam. The induced emittance growth from rf noise was shown to be a factor of 2 to 3 lower than predictions. The longitudinal impedance of the crab cavities was measured and found to agree with simulations.

In terms of the cavity beam dynamics, the bunch rotation was measured to be the expected 17 mrad. The nonlinear dynamics were investigated using turn-by-turn beam position monitors, to study the nonlinear coupling between the transverse planes resulting from the skew nature of the crab cavity. This analysis led to some course bounds on the skew-sextupole component of the cavity and further work is needed to disentangle the contribution of the crab cavity from the SPS optics nonlinearities, which play a dominant role over the faint signal induced by the crab cavity skew-sextupolar component. Further beam measurements are described in Refs. [33,34,36].

The major accomplishments made in this operation of a crab cavity in a hadron beam are a stepping stone toward the successful use of crab cavities for future colliders as the HL-LHC and opens the door to an era of high luminosity hadron beam physics.

TABLE I. Relevant rf and beam parameters for crab cavities in the HL-LHC and SPS tests.

Quantity	unit	HL-LHC	SPS-tests
Beam energy	GeV	7000	26–270
Frequency	MHz	400.79	400 [.528–.787]
Revolution frequency	kHz	11	43.3
Max. number of bunches		2760	288
Bunch length (4σ)	ns	1.0–1.2	1.8–2.6
Maximum cavity radius	mm	≤ 145	N.A.
Nominal kick voltage	MV	3.4	1.0 (in MDs)
R/Q (linac convention)	Ω	430	430
P_{dynamic} at 2 K, 3.4 MV	W	≤ 5	≤ 5
Q_{ext} (fixed coupling)		5×10^5	5×10^5
rf power (CW; 1 ms peak)	kW	(40; 80)	(40; 60)
LLRF loop delay	μs	≈ 1	≈ 1
Cavity detuning (if parked)	kHz	≈ 1.0	≈ 4.0

[1] O. Bruning *et al.*, LHC design report, Report No. CERN-2004-003-V-1, 2004, https://doi.org/10.5170/CERN-2004-003-V-1.

[2] A. Abada *et al.*, FCC-hh: The hadron collider: Future circular collider conceptual design report volume 3, Eur. Phys. J. Special Topics **228,** 4 (2019).

[3] M. Carlà, J. Beebe-Wang *et al.*, Electron Ion Collider Conceptual Design Report, EIC CDR, 2021.

[4] *High- Luminosity Large Hadron Collider (HL-LHC): Technical Design Report*, edited by I. Alonso, O. Bruning, P. Fessia, M. Lamont, L. Rossi, L. Tavian, and M. Zerlauth, CERN Yellow Reports: Monographs Vol. 10 (2020). ISBN 978-92-9083-587-5, https://doi.org/10.23731/CYRM-2020 -0010.

[5] W. Herr and B. Muratori, Concept of luminosity, CAS— CERN Accelerator School: Intermediate Course on Accelerator Physics, Zeuthen, Germany, 2003, pp. 361–378; Report No. CERN-2006-002. https://doi.org/10.5170/ CERN-2006-002.361

[6] A. Piwinski, DESY Report No. DESY 77/18, 1977.

[7] R. Palmer, Energy scaling, crab crossing and the pair problem, 4th DPF Summer Study on High-energy Physics in the 1990s, Snowmass, CO, USA, 27 Jun–15 Jul 1988, pp. 613–619.

[8] K. Oide and K. Yokoya, Phys. Rev. A **40,** 315 (1989).

[9] R. Calaga, Crab Cavities for the High-luminosity LHC, in *18th International Conference on rf Superconductivity (SRF2017)* (JACoW, Geneva, Switzerland, 2017), https:// doi.org/10.18429/JACoW-SRF2017-THXA03.

[10] K. Hosoyama *et al.*, *Superconducting crab cavity for KEKB, in the proceeding of APAC*, Tsukuba, 1998.

[11] Y. P. Sun, R. Assmann, J. Barranco, R. Tomas, T. Weiler, F. Zimmermann, R. Calaga, and A. Morita, Phys. Rev. ST Accel. Beams **12,** 101002 (2009).

[12] A. Chao and M. Tigner, *Handbook of Accelerator Physics and Engineering*, World Scientific, Singapore, 1999.

[13] R. Calaga, *in the proceedings of LHC performance workshop*, Chamonix, 2010.

[14] S. Verdu-Andres *et al.*, Design and vertical tests of double-quarter wave cavity prototypes for the high-luminosity LHC crab cavity system, Phys. Rev. Accel. Beams **21,** 082002 (2018).

[15] B. Xiao *et al.*, Design, prototyping, and testing of a compact superconducting double-quarter wave crab cavity, Phys. Rev. Accel. Beams **18,** 041004. (2015).

[16] A. Castilla *et al.*, First rf performance results for the DQW crab cavities to be tested in the CERN SPS, in *Proc. IPAC17*, Copenhagen, CERN-ACC-2017-283, 2017, https://doi.org/10.18429/JACoW-IPAC2017-MOPVA 095.

[17] C. Zanoni *et al.*, Design of dressed crab cavities for the HL-LHC Upgrade, *Proceedings, in Proc. of RF Superconductivity (SRF2015, THPB070), Whistler, 2015* (JACoW, Geneva, 2015), https://doi.org/10.18429/JA-CoW-SRF2015-THPB070.

[18] C. Zanoni *et al.*, The crab cavities cryomodule for SPS test, J. Phys. Conf. Ser. **874,** 012092 (2017).

[19] M. Sosin *et al.*, Position monitoring system for HL-LHC crab cavities, in *Proc. of IPAC16, Busan, 2016* (JACoW, Geneva, 2016), ISBN 978-3-95450-147-2.

[20] K. Artoos *et al.*, Development of SRF cavity tuners for CERN, in *Proceedings of the SRF 2015, Whistler, 2015* (JACoW, Geneva, 2015), https://doi.org/10.18429/JA-CoW-SRF2015-THPB060.

[21] K. Artoos *et al.*, Status of the HL-LHC crab cavity tuner, in *Proceedings of the SRF 2019, Dresden, 2019* (JACoW, Geneva, 2019), https://doi.org/10.18429/JACoW-SRF2019 -TUP081.

[22] L. R. Carver *et al.*, First machine development results with HL-LHC crab cavities in the SPS, in *Proc. of IPAC 2019* (JACoW, Geneva, 2019), pp. 338–341, MOPGW094, https://doi.org/10.18429/JACoW-IPAC2019 -MOPGW094.

[23] T. .E. Levens *et al.*, Automatic detection of transverse beam instabilitiesin the Large Hadron Collider, Phys. Rev. ST Accel. Beams **22,** 112803 (2019).

[24] J. Tuckmantel, Cavity beam transmitter interaction formula collection with derivation, CERN, Geneva, Report No. CERN-ATS-Note-2011-002-TECH, 2011.

[25] E. Yamakawa *et al.*, Beam loading study for HL-LHC and measurements in SPS crab cavities, STFC Internal Report-2018 (unpublished).

[26] K. Ohmi *et al.*, Response of colliding beam-beam system to harmonic excitation due to crab-cavity rf phase modulation, Phys. Rev. Accel. Beams **14,** 111003 (2011).

[27] L. Medina, R. Tomás, G. Arduini, and M. Napsuciale, Assessment of the performance of High Luminosity LHC operational scenarios: Integrated luminosity and effective pile-up density, Can. J. Phys. **97,** 498 (2018).

[28] F. Antoniou, A. Alekou, H. Bartosik, T. Bohl, R. Calaga, L. Carver, L. Repond, and G. Vandoni, Emittance growth in coast in the SPS at CERN. J. Phys. Conf. Ser. **1067,** 022008 (2018).

[29] J. Bosser, J. Camas, L. Evans, G. Ferioli, R. Hopkins, J. Mann, and O. Olsen, Nucl. Instrum. Methods Phys. Res., Sect. A **235,** 475 (1985).

[30] P. Baudrenghien and T. Mastoridis, Phys. Rev. Accel. Beams **18,** 101001 (2015).

[31] E. Shaposhnikova, Impedance effects during injection, energy ramp & store, *LHC-CC10 workshop* (CERN, Geneva, 2010); A. Burov *et al.*, Impedance aspects, *LHC-CC11 Workshop* (CERN, Geneva, 2011).

[32] N. Biancacci *et al.*, HL-LHC impedance and stability studies, *Proceedings of the 4th HiLumi-LHC workshop, KEK*, 2014.

[33] J. Mitchell, Ph. D. Dissertation, University of Lancaster, 2019, https://doi.org/10.17635/lancaster/thesis/743.

[34] M. Carlà, A. Alekou, H. Bartosik, and L. R. Carver, Beambased measurement of the skew-sextupolar component of the radio frequency field of a HL-LHC-type crab-cavity, CERN Report No. CERN-ACC-NOTE-2020-0024, 2020, https://cds.cern.ch/record/2715376.

[35] E. Cruz Alaniz, Y. Papaphilippou, and C. P. Welsch, RF multipoles deliverable, CERN Report No. CERN-ACC-NOTE-2020-0031, http://cds.cern.ch/record/2718290.

[36] A. Alekou, F. Antoniou, R. B. Appleby, H. Bartosik, R. Calaga, M. Carla, L. Carver, Y. Papaphilippou, and C. Welsch, Deliverable 2.7: Analysis of the existing sources of blow-up in the SPS by experiments and estimation/ measurement of the effect of the crab cavities in the SPS, CERN Report No. CERN-ACC-2020-0001, 2020, https:// cds.cern.ch/record/2706139/files/CERN-ACC-2020-0001 .pdf.